Mol. Cryst. Liq. Cryst., Vol. 420, pp. 9–33, 2004
Copyright © Taylor & Francis Inc.
ISSN: 1542-1406 print/1563-5287 online
DOI: 10.1080/15421400490487416

Taylor & Francis
Taylor & Francis Group

EFFECT OF THE THERMAL HISTORY ON THE THERMAL AND RHEOLOGICAL BEHAVIOR OF A THERMOTROPIC POLYESTER

*Jorge A. Ressia, Lidia M. Quinzani, and Enrique M. Valles**
Planta Piloto de Ingeniería Química—PLAPIQUI (UNS-CONICET), Bahía Blanca, Argentina

Pablo Bello and Antonio Bello
Instituto de Ciencia y Tecnología de Polímeros (CSCIC), Madrid, Spain

The biphasic behavior and phase transitions of a thermotropic main-chain liquid crystalline polyester, the poly(oxytrimetilen-etilen glycol p,p′-bibenzoate), was studied by X-ray diffractometry, differential scanning calorimetry (DSC), and rotational rheometry. The liquid crystalline mesophase structure of the polymer evolves from Smectic C to Smectic A at around 100°C and changes to the isotropic state at about 200°C. The annealing of polymer samples at different temperatures within the smectic–isotropic transition gives rise to double endotherm and exotherm peaks on the heating and cooling DSC traces. These peaks are attributed to the preferential segregation of the lower molecular weight molecules from the liquid crystalline to the isotropic phase in the biphasic zone. The rheological studies are consistent with this result. The dynamic moduli measured at constant frequency in temperature ramps using polymer samples with different thermal histories reveal that the type of annealing processes applied in the biphasic zone generates different evolution of the rheological data.

Keywords: thermotropic; liquid crystal; segregation; rheology

The authors thank the CICYT, Spain (grant MAT2001-800X-711), the *National Research Council* (CONICET), the *Buenos Aires Scientific Commission* (CIC), and the *Universidad Nacional del Sur* (UNS), Argentina, for their financial support. We also wish to thank the collaboration of A. del Campo and E. Pérez for the synchrotron measurements.

*Corresponding author. E-mail: valles@plapiqui.edu.ar

INTRODUCTION

The analysis of the phase transitions of thermotropic main-chain liquid crystalline polymers (LCPs) is a topic of great interest. There are several factors that influence the anisotropic–isotropic phase transition of these materials, making the interpretation of this phenomenon much more complex than that of their low molecular weight counterparts. For thermotropic LCPs, the biphase structure that occurs during the anisotropic–isotropic transition may remain stable at thermal equilibrium over a certain temperature interval. This behavior has been observed for several nematic LCPs with chemically regular structures and was attributed to the polydispersity in the molecular mass [1–10]. For some of these polymers, it has been demonstrated that the chains are preferentially distributed in the isotropic and anisotropic phases of the biphasic region according to their length. Longer chains are more stable in the liquid crystalline phase, while shorter molecules tend to migrate to the isotropic domains. Consequently, the thermal history applied to a thermotropic polymer in the biphasic zone may severely affect the organization and composition of the different domains, influencing the morphology and rheological properties of these materials.

In consideration of the scientific connotations of this important phenomenon, we have studied the thermal and the viscoelastic properties of a main-chain LCP of the Smectic type in the vicinity of the biphase region. The polymer analyzed in the present study is a poly(oxytrimetilen-etilen glycol p,p′-bibenzoate) (PETB). The structural unit of this polymer shown in Scheme 1.

The asymmetric structure of the spacer in this polymer generates a material with relatively low melting and clearing temperatures. This characteristic facilitates the execution of the necessary experiments to characterize the polymer well below the higher temperatures where the chemical alterations and decompositions begin to be important.

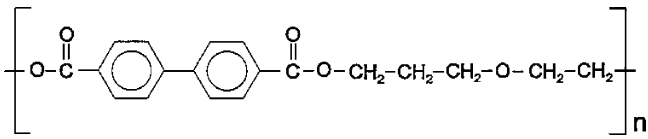

SCHEME 1

EXPERIMENTAL SECTION

Synthesis

The synthesis of the ether-diol, $HO-CH_2-CH_2-O-CH_2-CH_2-CH_2-OH$, was done at room temperature under nitrogen atmosphere by slowly adding oxetane to an excess of ethylene glycol using sulfuric acid as catalyst. In a typical reaction, 0.1 mol of sulfuric acid was slowly dissolved in 1.5 mol of ethylene glycol contained in a round-bottom flask cooled with water. In a second step, 0.15 mol of purified oxetane was added dropwise to this solution during a period of nearly 2 h. The reaction was terminated with sodium bicarbonate. The product was filtered, washed with water, extracted with chloroform, and distilled several times under vacuum. The yield of ether-diol was close to 80%.

The synthesis of diethyl p,p′-bibenzoate was performed in two steps. In the first one, 0.6 mol of thionyl chloride was added dropwise, under ice cooling, to 0.1 mol of p,p′-bibenzoic acid. Pyridine was then added as catalyst, and the reaction mixture was stirred at 60°C for 10 h. The p,p′-bibenzoyl dichloride formed was separated by filtration and washed with dry benzene. In the second step, diethyl p,p′-bibenzoate (DB) was rapidly obtained by addition at room temperature of an EtNa/EtOH solution to the p,p′-bibenzoyl dichloride. The solvent was then eliminated at reduced pressure, and the synthesized DB was dissolved in chloroform and washed with water. After drying with $MgSO_4$, the chloroform was removed at reduced pressure and the ester was recrystallized from ethanol. The yield of DB was 67%.

The polyester PETB was obtained by melt transesterification of the previously synthesized DB and ether-diol using tetraisopropyl titanate (TIPT) as catalyst. The procedure was as follows: First, a mixture of DB (0.1 mol) and ether-glycol (0.12 mol) was heated at 190–200°C under stirring. Then, 0.03 ml of TIPT were added to the mixture, which was stirred under nitrogen atmosphere for 3 h. Finally, the polycondensation was carried out at higher temperature (200–250°C) under reduced pressure (0.01 mmHg) for 2 h. After cooling, the polymer was dissolved in chloroform, precipitated with methanol, and finally dried in an oven.

Characterization

Size exclusion chromatography (SEC) was performed in a Waters 150-C apparatus. The chromatograms were obtained at 30°C using a set of PLgel columns (two mixed bed of 5μ) and chloroform as the solvent. A dual detector system, differential refractometer and viscometer (Viscotek 150 R), working at 30°C was connected to the columns. The conditions used

in the experiments were: a flow rate of 1.0 ml/min and a sample concentration of 5 mg/ml. The system was calibrated with twelve polystyrene samples of narrow molecular weights, considering the M_{peak} as representative of the whole sample. Corrections for band broadening and viscometer offset were done using a polystyrene sample of broad and known molecular weight distribution employing standard procedures. The universal calibration method was used to determine the distribution of molecular weights of the polyester and the number- and weight-average molecular weights.

Wide-angle X-ray diffraction (WAXD) photographs were taken with a flat-plate camera attached to a Phillips 2 kW tube X-ray generator using a sample film distance of 7 cm. Nickel-filtered CuKα radiation was used in all cases. Unoriented polymer films for X-ray measurements were prepared in a heated press fitted with Teflon plates. The polymer samples were hot pressed above the isotropization temperature for 5 min and then cooled at constant pressure by quenching the films between the two water-cooled plates. Fibers were then obtained by stretching a piece of the thermotropic polyester film at a temperature just slightly above T_g. The drawing (or stretching) ratios were close to 1:6.

Synchrotron radiation ($\lambda = 0.150$ nm) performed in the beamline A2 at HASYLAB (Hamburg, Germany) was employed to make additional X-ray scattering experiments. For this purpose, film samples of about 20 mg were covered by aluminum foil to ensure homogeneous heating or cooling and placed in the temperature controller of the line under vacuum. Heating or cooling experiments were performed at rates of 2 or 4°C/min. More experimental details are given in Pérez et al. [11].

The texture of the polymer was observed with a Carl-Zeiss microscope equipped with crossed polarizers. The samples were placed in a heating-cooling stage from Mettler, and the gradual change of the polymer texture was followed as a function of temperature.

The thermal transitions were determined by differential scanning calorimetry (DSC) under dry nitrogen flow using a DSC Pyris I system from Perkin Elmer. Temperature and enthalpy calibrations were carried out using analytical-grade indium as a reference. Polymer samples of 5–10 mg were employed. A preliminary scan was performed on each analyzed specimen to make the thermal history uniform. This scan consisted of heating the samples at 40°C/min up to 220°C, well beyond the isotropization temperature, and maintaining that temperature for 20 min. The samples were then cooled down to 100°C at 5°C/min. This scan is referred to in this article as the "reference scan." As will be shown later in this article, this preliminary scan does not ensure that the thermal history of the samples is completely erased.

Regular scans were performed after the reference scans, heating the samples from 100°C up to 220°C at a rate of 10°C/min to determine the isotropization temperature, T_l, and the enthalpy corresponding to the transition from the mesophase to the isotropic state, ΔH_l. Afterwards, the samples were kept at 220°C for 20 min and cooled back to 100°C at 5°C/min to obtain the enthalpy and the temperature of the maximum of the exothermic peak through the isotropic-liquid-crystalline transition, ΔH_c and T_c. These peaks are referred in this article as the "original endotherm" and the "original exotherm," respectively.

More complex heating patterns were adopted to characterize the thermal behavior of the polymer in the biphasic zone. They are schematized in Figure 1. As was previously explained, after running the reference scan some samples were subjected to an annealing process according to the following program: (1) the sample was heated from 100°C to the annealing temperature, T_A, at 10°C/min and kept at this temperature during a period of time t_A; (2) the temperature was slowly reduced up to T_s at a rate of 1°C/min and kept at that value for a period of time t_s; (3) the sample was then heated to 220°C at 5°C/min and maintained at that temperature for 20 min; and (4) the temperature was reduced to 100°C at a rate of 5°C/min. The values of the reference temperatures and length of times used are reported in Table I. A few specific runs in which the samples were kept in the molten state at 220°C for more than 20 min are discussed later in this article. In some cases, the previously described cycle was applied several consecutive times to the same sample increasing the time t_s progressively.

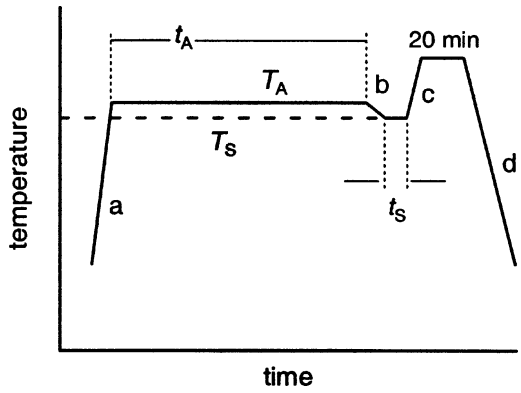

FIGURE 1 Schemes of the temperature programs used in the DSC tests. Heating/cooling rates: a, 10°C/min; b, 1°C/min; c, 5°C/min; d, 5°C/min.

TABLE I Temperatures and Times Used in the Different Steps of the Annealing Tests Performed in the DSC

Maximum temperature	Minimum temperature	Annealing temperature (T_A)	Time of annealing (t_A)	Stepping temperature (T_s)	Time of step (t_s)
220	100	192, 194, 196	120[a]	185	0, 2, 10, 30[b]

Temperatures are reported in °C and times in min.
[a] Except in the cases mentioned in the text.
[b] $t_s = 0$ means that the sample was immediately heated after it reached T_s.

A final complete heating and cooling cycle, from 100 to 220°C and from 220 to 100°C, was applied to the studied annealed samples. The endothermic and exothermic peaks generated during this final cycle, at the end of the whole test, are referred as the "final endotherm" and the "final exotherm," respectively. The results of this cycle were used to analyze the remaining effect of the applied thermal histories by comparison of the final values of the transition temperatures and enthalpies with those of the original fresh samples. Fresh material was used in each annealing test.

Polymer Fractionation

A sample of the original PETB was separated in three portions of different molecular weight by fractional precipitation. The process was carried out in a fractionation flask at room temperature using chloroform as solvent and acetone as a nonsolvent. The original sample was dissolved in chloroform to form a 2 wt% solution. The acetone was then slowly added, drop by drop, to the constantly stirred solution until a permanent turbidity was achieved. The solution was at that time heated with an electric hot air blower until the solution was completely transparent. The content of the flask was then slowly cooled to room temperature under constant agitation. The turbid solution was allowed to ripen with no agitation for several hours, and the precipitated fraction, containing mainly the large molecular weight molecules, was separated from the funnel. The process was repeated a second time to obtain a fraction of intermediate molecular weight. The molecules of lower molecular weight remained in the solution and were finally precipitated with an excess of acetone. The fractions were washed and dried until the solvent and nonsolvent were removed completely.

Rheological Characterization

The rheological characterization was carried out in a rotational spectrometer RDA-II from Rheometrics Scientific. The rheometer was equipped

with a parallel plate fixture of 25 mm diameter and was operated under nitrogen atmosphere using small-amplitude oscillatory shear flow test. As in the calorimetric studies, and previous to any rheological test, the samples were placed in the rheometer, heated to 220°C, and kept at this temperature for 20 min to uniform the thermal history. The samples were then slowly cooled down (at approximately 2°C/min) to the testing temperature. Two types of rheological tests were used: (1) dynamic frequency sweeps (DFS) to obtain the elastic (G') and viscous (G'') moduli at different constant temperatures in the frequency range from 0.1 to 400 s^{-1}, and (2) temperature ramps (TR) to measure the dynamic moduli as a function of temperature at a constant frequency of 1 s^{-1}. The TR tests were applied heating the samples from an initial temperature of 170–220°C and then cooling back to the initial temperature. Both ramps were carried out at a rate of 1°C/min. Equivalent TR tests were applied to samples previously annealed during 2 and 4 h at 194°C. An additional test was carried out, consisting of a series of DFS runs performed at 194°C during a period of 3 h on a sample previously subjected to a DFS at 170°C. Finally, another DFS test was applied at 170°C to analyze the influence of the isothermal annealing at 194°C.

Strain sweep tests were initially carried out at several frequencies and temperatures in order to locate the zone of the linear viscoelastic response of the polymer at the different conditions [12]. Different strains were selected to perform the DFS at the various chosen temperatures; they will be mentioned in this article. A strain of 5% was used in the TR tests performed. Since several of the described rheological experiments were performed with only one sample using different temperatures, it was necessary to consider the change in size of the gap due to the thermal expansion of the plates. Consequently, special attention was adopted in adjusting and correcting the relative position of the plates in the rheometer when changing the temperature.

RESULTS AND DISCUSSION

Figure 2 shows the variation of the position of the maximum peak from MAXD, X-ray diffraction measurements, indicating the changes of the smectic spacing of the LCP with temperature. It also includes two X-ray photographs of fiber diffraction patterns, one obtained at room temperature and the other at 160°C. The specimens employed in both cases were prepared by elongation of the polymer at room temperature, using deformation rates that induce orientation of the polymer chains parallel to the drawing direction [13–16]. The diffraction pattern of the high temperature image is typical of a S_A mesophase, where the diffraction spots of the

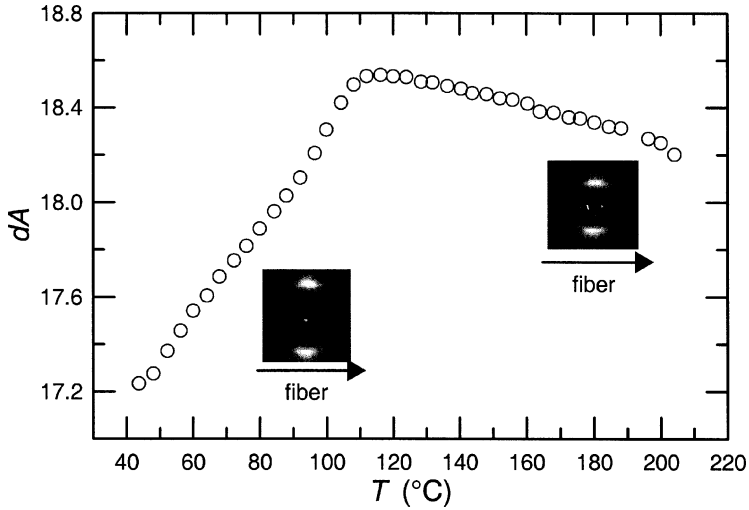

FIGURE 2 Variation of the position of middle-angle X-ray scattering (MAXS) peak as a function of temperature in a cooling experiment performed using a rate of 4°C/min, and WAXD photographs of the diffraction diagram of PETB fibers at 30 and 160°C.

smectic layers appear in the meridian, while the diffractions corresponding to the intermolecular distances are broad, with the maximum of intensity centered in the equator. The diffraction spectrum changes at low temperatures. Here the diffraction of the smectic spacing is divided into four spots displaced from the meridian position by an angle of 25°, while those corresponding to the liquid character of the mesophase remain with their maximum in the equator. The characteristics of the diffraction pattern correspond now to a S_C mesophase. Some additional aspects of the liquid crystalline structure of PETB have been reported previously [13].

The variation of the smectic spacing with temperature obtained with the synchrotron radiation technique allows a better picture of the influence of temperature on the type of mesophase. Two different regions are clearly distinguished in the plot: one from room temperature up to 100°C, where the temperature coefficient of the smectic spacing becomes remarkably positive; and the other from 100 up to 200°C, where the temperature coefficient of the smectic spacing is negative. In the high temperature region the spacing decreases with increasing temperatures. This is an indication that the less-extended gauche conformations are favored as the temperature is raised within the range of 100–200°C. A different behavior is observed in the region from 40 to 100°C. Here, besides any possible change in the conformation of the molecules due to the temperature, a new

smectic S_C mesophase appears, as it is demonstrated by the corresponding photography of the fiber diffraction pattern. The principal characteristic of this mesophase is that the chain axis and the smectic planes are not normal but tilted, forming an angle of 25° at room temperature. As the synchrotron data demonstrate, this angle diminishes as the temperature increases, becoming normal at temperatures in the surroundings of 100°C, where the S_A mesophase formation begins.

When a sample is molten in the DSC, immediately cooled to ice temperature at a rate of 10°C/min and then reheated at the same speed, only two transitions appear on heating: T_g at 25°C and T_1 at 198°C. This result indicates that, in the sequence of phase structures adopted by the sample from the molten state, i.e., isotropic, S_A, and then S_C, the transition from one type of mesophase to the other is of second order. Therefore, in the time scale used in the thermal and rheological experiments reported in this work, no other phase appears. Furthermore, in the temperature interval used in this work (100–200°C) only the S_A mesophase exists.

Thermal Analysis and Optical Microscopy

During a complete heating–cooling cycle between 0 and 220°C, the glass transition (T_g) of the polymer was detected at 25°C. The average isotropization temperature and the temperature corresponding to the transition from the isotropic melt to the liquid crystalline state were located from the position of the maximum and minimum of the endothermic and exothermic peaks, respectively. The values of those temperatures, as well as the associated enthalpies, are listed in Table II. The isotropization process occurs in a temperature gap of about 22°C, where evidences of a biphasic organization were found, as we explain below. An enthalpy of 19,800 J/kg was calculated from the endotherm of PETB on the heating cycle. This value is typical of liquid-crystalline-isotropic transitions of LCPs of the smectic type.

TABLE II Molecular Weights and Melting and Crystallization Temperatures of the Original Polymer and Three Fractions of PETB

Sample	M_n (g/mol)	M_w (g/mol)	T_1 (°C)	ΔH_1 (J/kg)	T_c (°C)	ΔH_c (J/kg)
Original PETB	6,500	14,800	198	19,800	189	19,100
Fraction 1	14,500	23,800	199	18,900	189	17,600
Fraction 2	9,800	12,100	196	19,300	188	17,000
Fraction 3	6,400	7,700	185	20,000	174	14,100

Figures 3 to 5 show the thermograms obtained in successive isothermal annealing tests applied to PETB in the transition zone. The type of thermal treatment used was already described in the Experimental Section. Table I lists the annealing temperatures and stepping times employed in the experiments. The results shown in each figure were obtained in consecutive thermal cycles applied to a given specimen. Fresh material was used in each series of scans, at $T_A = 192$, 194, and 196°C. The elapsed time t_s that the sample was kept at the temperature T_S in each cycle was successively increased. The selected annealing temperatures are located at intermediate positions between the temperatures that define the initiation and the completion of the isotropization process. The annealing process within the biphasic zone gives rise to double endotherm and exotherm peaks on the heating and cooling DSC traces. The maxima of these two peaks are located at a lower and higher temperature, respectively, than that corresponding to the maximum of the original endotherm. Equivalently, the minima of the exotherms in the cooling process are also located at lower and higher temperatures than the original one. The relative position of the maximum of the two endotherm peaks generated on the heating process, which are called peak 1 and peak 2, respectively, increases slightly with t_s, as shown in Figure 6 for $t_s = 0$ min and $t_s = 30$ min. This implies that sufficiently long times should be given to the fraction of the polymer that has reached the isotropic state during the annealing process at T_A to complete the transition back to the liquid crystalline phase when the polymer temperature is lowered to T_s.

The temperature at which the maxima of the endotherms are reached increase significantly with the annealing temperature. Figure 6 reveals that a shift of approximately 2°C occurs for both peaks as T_A is raised from 192 to 194°C. The relative heights and areas of both peaks also change with T_A. As is shown in the thermograms, the height of peak 1 increases while that of peak 2 decreases when the annealing temperature augments. The height is calculated from peaks that are normalized in each scan to obtain the same total area under the thermograms.

To complement the DSC studies, the phase-separation process of PETB that occurs during the transition was observed by polarizing light microscopy using cross polarizers and a red filter between them. When annealing experiments were performed on the hot stage of the microscope at the same temperatures that are used in the DSC experiments, a clear distinction between the isotropic melt and the liquid crystalline phase was observed. The portions of isotropic and liquid crystalline polymer remain stable for long periods of time, demonstrating the stability of the biphasic region. As T_A was increased, the area occupied by the isotropic phase visualized in the microscope was significantly modified. At temperatures close to 192°C, segregated droplets of isotropic melt were observed in

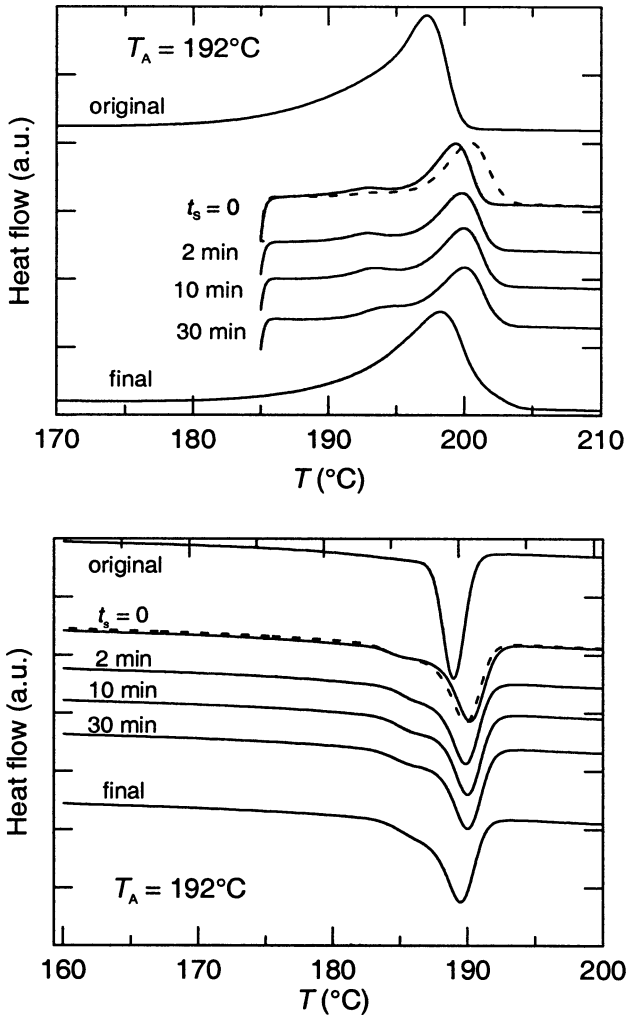

FIGURE 3 DSC traces corresponding to the melting and crystallization transitions of PETB annealed at 192°C in successive cycles with different stepping times at 185°C. The stepping time (shown next to each trace) was gradually increased from one cycle to the next. The dotted line corresponds to a last annealing cycle with $t_s = 0$. The original (second cycle) and final (final cycle) endotherms are also included.

a continuous liquid crystalline phase. In contrast, close to 198°C the structure of the polymer sample showed disperse mesogenic domains in a continuous isotropic phase.

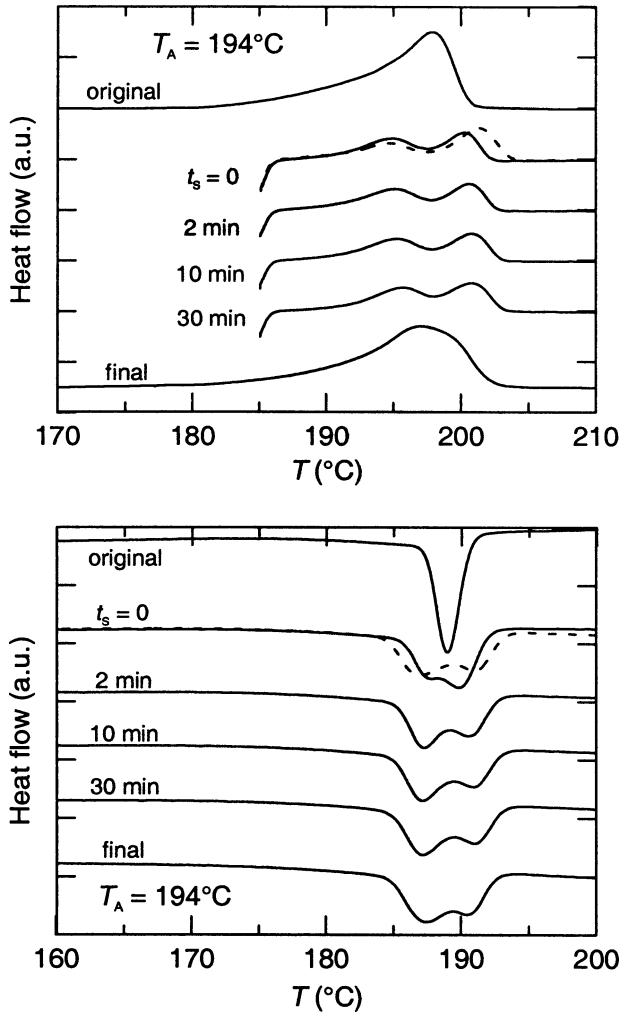

FIGURE 4 DSC traces corresponding to the melting and crystallization transitions of PETB annealed at 194°C in successive cycles with different stepping times at 185°C. The stepping time (shown next to each trace) was gradually increased from one cycle to the next. The dotted line corresponds to a last annealing cycle with $t_s = 0$. The original (second cycle) and final (final cycle) endotherms are also included.

The invariance of the results at long times—both in the DSC experiments and in the optical observations—throughout extensive annealing processes confirms that the isotropic and smectic phases generated by

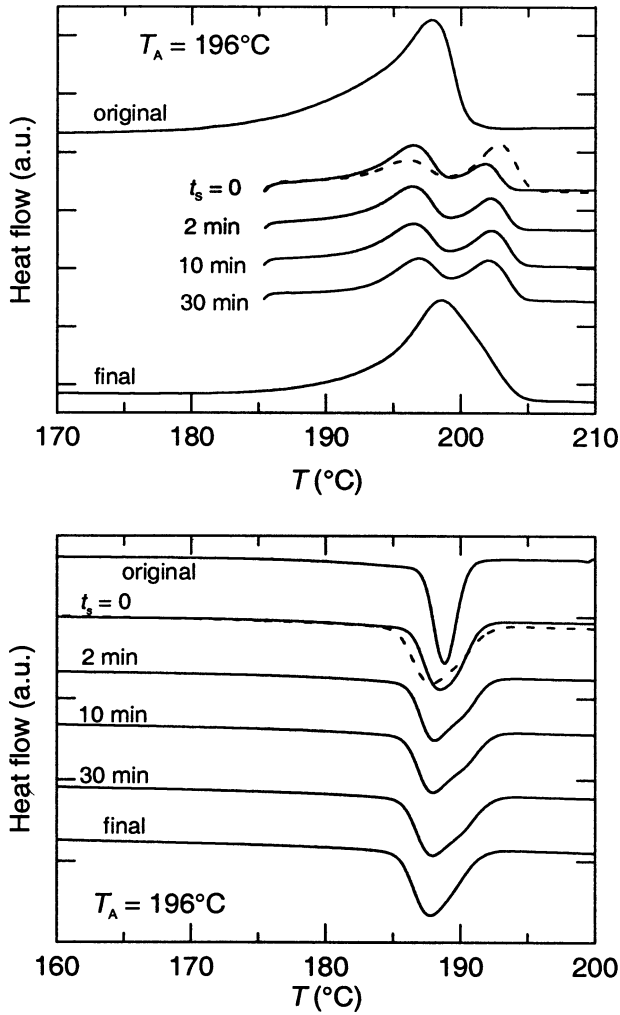

FIGURE 5 DSC traces corresponding to the melting and crystallization transitions of PETB annealed at 196°C in successive cycles with different stepping times at 185°C. The stepping time (shown next to each trace) was gradually increased from one cycle to the next. The dotted line corresponds to a last annealing cycle with $t_s = 0$. The original (second cycle) and final (final cycle) endotherms are also included.

maintaining the polymer at a constant temperature within the zone of the liquid-crystalline-isotropic transition coexist at equilibrium. This behavior is consistent with a segregation of the polymer molecules according to

molecular weight as has been observed in other thermotropic main-chain LCPs [7–9]. During the annealing process, the shorter polymer chains are segregated preferentially out of the liquid crystalline phase to form isotropic domains in which the molecules are expected to be in essentially random-coiled configurations. The change of the temperature of the maxima and the relative magnitudes of peaks 1 and 2 with T_A is consistent with this explanation. A higher T_A includes biphases with more extensive domains of isotropic low molecular weight material, which increases the magnitude of peak 1 to the detriment of the high temperature peak. In these conditions only the molecules of larger molecular weight could remain in extended-chain conformation compatible with the smectic configuration. This molecular migration of the lower molecular weight molecules from the liquid crystalline phase to the isotropic state results in the shifting of the maximum of peak 2 towards higher temperatures.

In the calorimetric tests, the cooling process from the isotropic melt was always initiated after holding the polymer at 220°C for at least 20 min. The

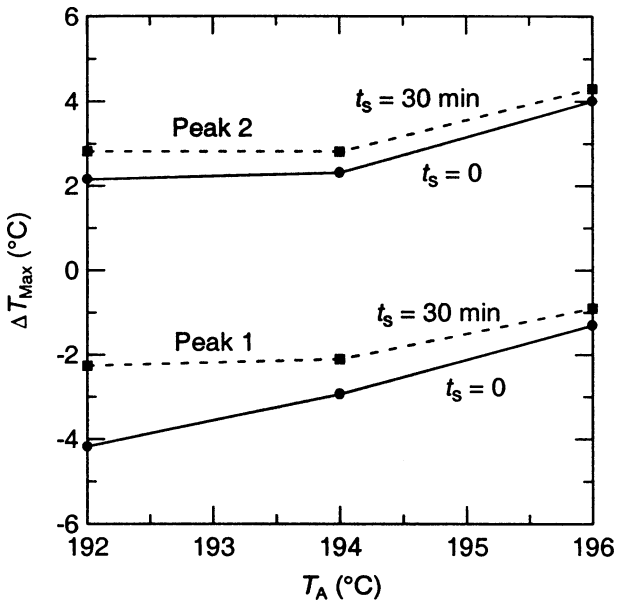

FIGURE 6 Maximum temperatures of the normalized endotherms relative to the isotropization temperature of PETB as a function of the annealing temperature for $t_s = 0$ and 30 min. Peaks 1 and 2 are those observed at the lower and higher temperatures, respectively.

onset of the transition from isotropic to smectic organization occurs with a supercooling of about 12°C. Probably the most interesting feature of the exotherms obtained at this step is that the time of permanence at 220°C is clearly not sufficient to erase the history induced by the annealing processes since two peaks are invariably observed in the cooling cycle of the previously annealed samples. The persistent presence of the two exothermic peaks is a clear indication that the segregation of the molecules by molecular weight during the previous annealing process can prevail for long periods of time. This is clearly demonstrated throughout the series of exotherms shown in Figure 7. They were obtained by taking the sample annealed at 194°C that was used in the series of scans illustrated in Figure 4 and successively heating it from 100 to 220°C at 10°C/min, letting it stay at 220°C for 20 min, and cooling it from 220 to 100°C at 5°C/min through several cycles. The two scans on top of Figure 7, which are labeled as "original" and "final," are the initial and last runs, respectively, of the annealing experiments already shown in Figure 4. The other four scans in the figure show the evolution of the variation of the endothermic and exothermic peaks of the "final" segregated polymer with successive heating and cooling cycles. The thermograms show that the double peaks are progressively less noticeable. Nevertheless, they still can be clearly appreciated in the last exotherm, after 100 min of accumulative time in the molten state. It is evident that the segregation of the polymer molecules during the annealing process can prevail in the isotropic state for long periods of time. This fact suggests that strong "memory effects" are generated by the segregation process and that the diffusion process of molecules between phases is comparatively slow, keeping the molecules segregated for long periods of time.

In order to verify the influence of the molecular weight on the location and characteristics of the biphase region, a sample of the original PETB was fractionated in three portions of different molecular weight by fractional precipitation, as indicated. The SEC chromatograms and the DSC scans corresponding to the three fractions of different molecular weight are shown in Figures 8 and 9, respectively. The average molecular weights and the more significant features of the DSC scans are summarized in Table II. As expected, both in the heating and cooling cycles, the maxima and the initial and final temperatures of the peaks decrease as the molecular weight of the fractions decreases. The original endotherm and exotherm of PETB have their maximum temperatures between those of fractions 1 and 2. It is interesting to notice that the range over which the thermal transition of the low molecular weight fraction takes place is about 60°C on the heating cycle and slightly more than 50°C in the cooling process. This is roughly three times the range corresponding to the two other higher molecular weight fractions. The maxima of the heating and

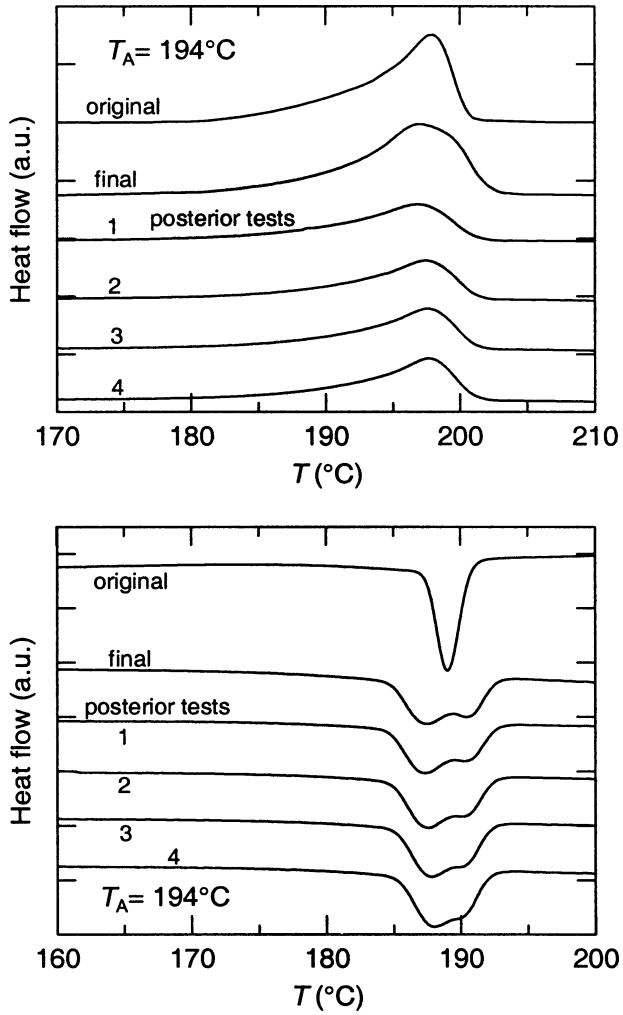

FIGURE 7 Endotherms and exotherms corresponding to the isotropic liquid crystalline transition of the PETB previously subjected to an annealing test at 194°C. The original and final curves are the same as those shown in Figure 4. The remainder of the curves are the DSC traces obtained in successive cycles of heating and cooling performed after the final one.

cooling cycles of the low molecular weight fraction are also considerably apart from those of the original polymer and the high molecular weight fractions. In contrast, the magnitudes of the transition enthalpies for the three fractions do not seem to change significantly with molecular weight.

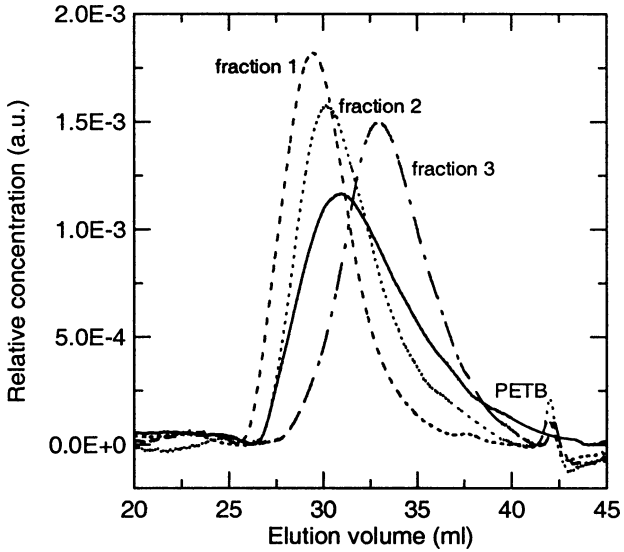

FIGURE 8 Chromatograms of the original PEBT and the three fractions obtained by fractional precipitation. Lines: solid, PETB; short-dashed, fraction 1; dotted, fraction 2; long-dashed, fraction 3.

Rheological Characterization

Figure 10 shows the dynamic moduli of PETB measured at selected temperatures. The samples were initially melted at 220°C and kept at this temperature for 20 min. Elapsed this time, a DFS test was applied at that temperature to the molten polymer using a 10% strain. The temperature was then reduced to 170°C at a rate of $\sim$2°C/min, below the isotropization transition, and a DFS was applied to the sample using a 1% strain. Finally, the temperature was increased to an intermediate value (194°C), and a DFS was performed with 1% strain. The elastic and the viscous moduli of PETB increase as the temperature decreases, with G' augmenting in a large proportion. This effect is expected since, in the range of temperatures analyzed, the polymer goes from an isotropic molten condition to the quasi-solid state. At 220°C, the behavior is typical of conventional flexible polymer melts, which exhibit a viscous modulus dominating in the low frequency regime [17]. At lower temperatures, the effect of the molecular organization and the presence of multiphases may be appreciated at low frequencies [12,18]. The relatively large values of $G'(\omega)$ in this region (larger than those of $G''(\omega)$ at 170°C) indicate the presence of a weak structure that has a rheological behavior akin to lightly cross-linked or gel-like materials [17]. The deformation of this type of polymer during flow

involves an extra energy that contributes mainly to the stored elastic energy, that is, to G'.

A detailed study of the effect of the annealing time was done at 194°C. As was already mentioned in the Experimental Section, periodic DFS tests

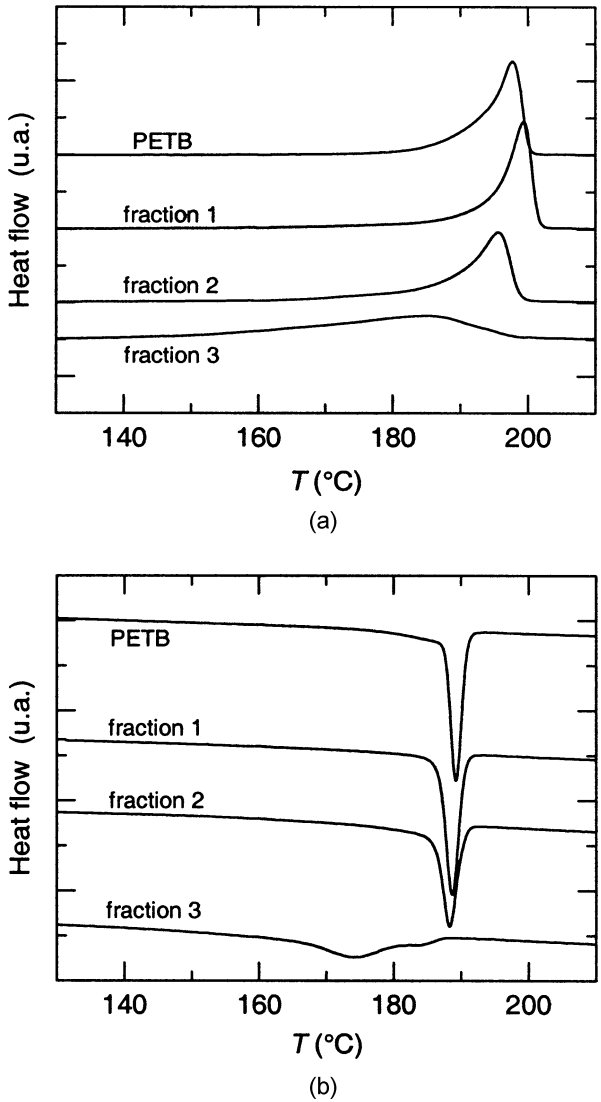

FIGURE 9 DSC traces of the (a) heating and (b) cooling cycles of the original PETB and the three fractions separated by fractional precipitation.

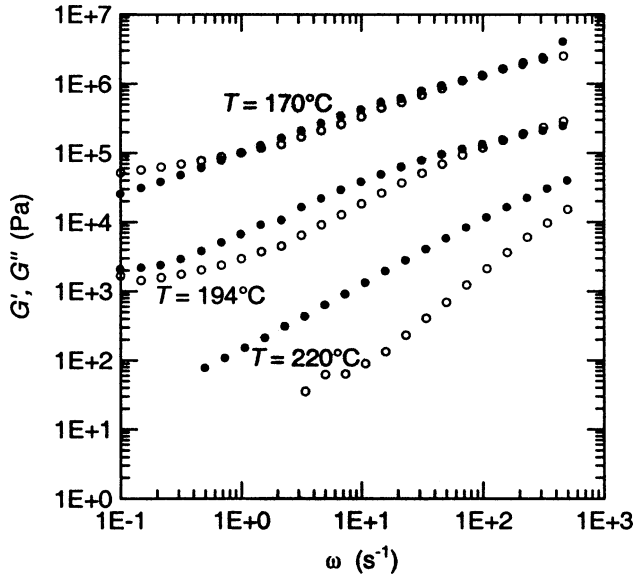

FIGURE 10 Elastic (G') and viscous (G'') moduli of PETB as a function of frequency measured at 170, 194, and 220°C and strains of 1, 1, and 10%, respectively. Symbols: (○), G'; (●), G''.

were applied during a total period of 3 h to a sample kept at constant temperature. Figure 11 shows the dynamic moduli of PETB measured at different annealing times t_A. The first run, performed immediately after the sample reached 194°C, is identified as $t_A = 0$. The following tests were performed 30, 60, 120, and 180 min later. It may be observed that the molecular reorganization produced during the isothermal annealing affects the dynamic moduli, which decrease with the annealing time. The rheological data after 120 and 180 min of annealing are very similar, showing that the polymer sample is reaching the final molecular reorganization. The low molecular weight molecules that migrate from the liquid crystalline domains to the isotropic region during the annealing process reduce the size of those domains with the associated reduction in interfacial area and the viscosity of the surroundings of the oriented domains with the associated lubrication effect. These effects may explain the observed decrease of both moduli. The reaction of the elastic modulus is larger because this modulus is more affected by the area of the interface than the viscous one.

As described in the Experimental Section, an additional DFS test at 170°C was performed to the sample annealed at 194°C for 3 h. When the

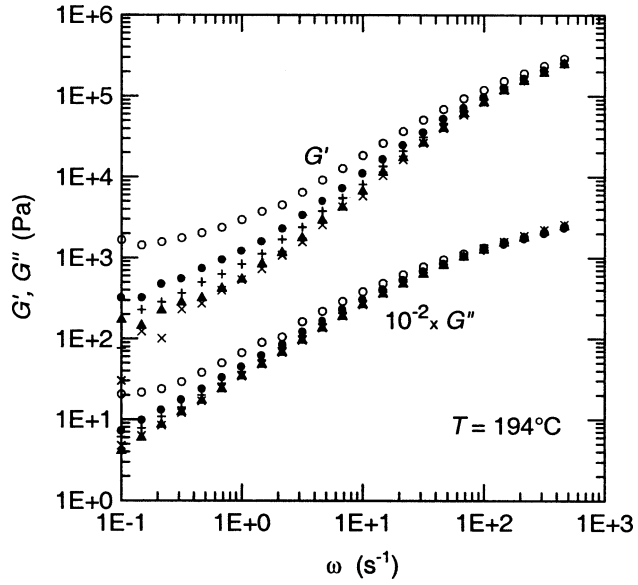

FIGURE 11 Elastic (G') and viscous (G'') moduli of PETB as a function of frequency measured at 194°C after different annealing times (t_A). Symbols: $t_A = 0$(○), 30(●), 60(+), 120(▲), and 180(×) min.

experience described in the previous paragraph was finished, the material was heated in the rheometer to 220°C, kept at that temperature for 20 min, and finally cooled back to 170°C, where a final DFS was performed. Figure 12 compares the moduli G' and G'' measured at 170°C in the two finals DFS (before and after the sample was heated to 220°C) with those obtained in the initial run applied to the sample with no annealing (already shown in Figure 10). The decrease in the viscoelastic parameters observed after the annealing process is in accordance with the results at 194°C shown in Figure 11. Additionally, it is interesting to observe that the final elastic and viscous modulus curves, obtained after the 20 min of keeping the polymer in the molten state, are very similar to the initial ones, even considering the accumulative error produced by the many times that the gap between the plates had to be adjusted by the time this test was finished. According to this result, the recuperation of the original molecular spatial distribution seems to be faster in the rheological test than in the calorimetric tests. A reason for this may be that the rheological tests involve deformation of the material and relative displacement of the polymer molecules. The imposed flow has a mixing effect that may help to recuperate the initial distribution.

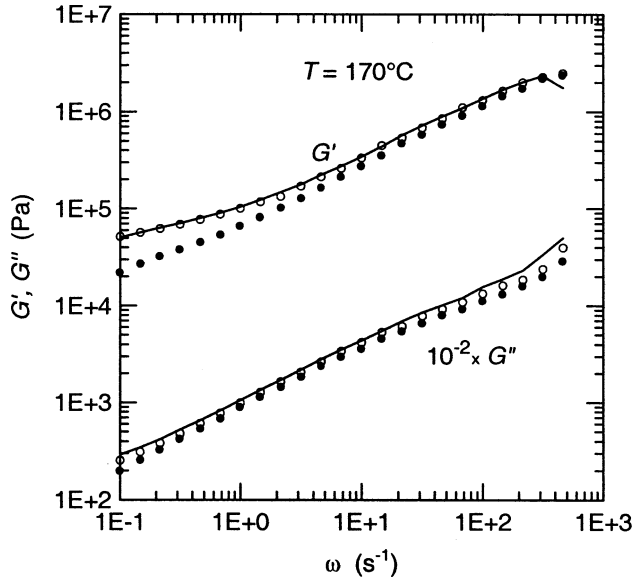

FIGURE 12 Elastic (G') and viscous (G'') moduli of PETB as a function of frequency measured at 170°C on the same sample after different thermal histories. Symbols: (○), after melting the fresh sample at 220°C; (●), after 180 min of annealing at 194°C; (solid line), after the 180 min of annealing at 194°C followed by melting at 220°C.

More revealing tests are the cycles of TRs with simultaneous application of oscillatory shear flow. In all of the cases, the heating and cooling rates applied were 1°C/min, the frequency $1\,s^{-1}$, and the strain 5%. The dynamic moduli were measured in both the heating and cooling ramps with time steps of 1 min. Each test consisted of three consecutive cycles. During the first cycle, the fresh sample is heated from a low temperature to 220°C, kept at this temperature during 20 min, and then cooled back up to 170°C. Second and third similar cycles were performed between 170 and 220°C after the sample was previously subjected to 2 and 4 h, respectively, of isothermal annealing at 194°C. Figure 13 shows the elastic and the viscous modulus obtained during the three cycles. During the first heating TR the behavior of the moduli with temperature is typical of a polymer that goes from the solid to the molten state. The dynamic moduli decrease to very low values, with a sharp decrease occurring during the period in which the isotropization takes place (approximately 185–203°C). Equivalently, during the first cooling TR the dynamic moduli increase monotonically. Sharp raises of the viscoelastic parameters are observed to initiate at 193°C, where the transition to the liquid crystalline phase begins to take

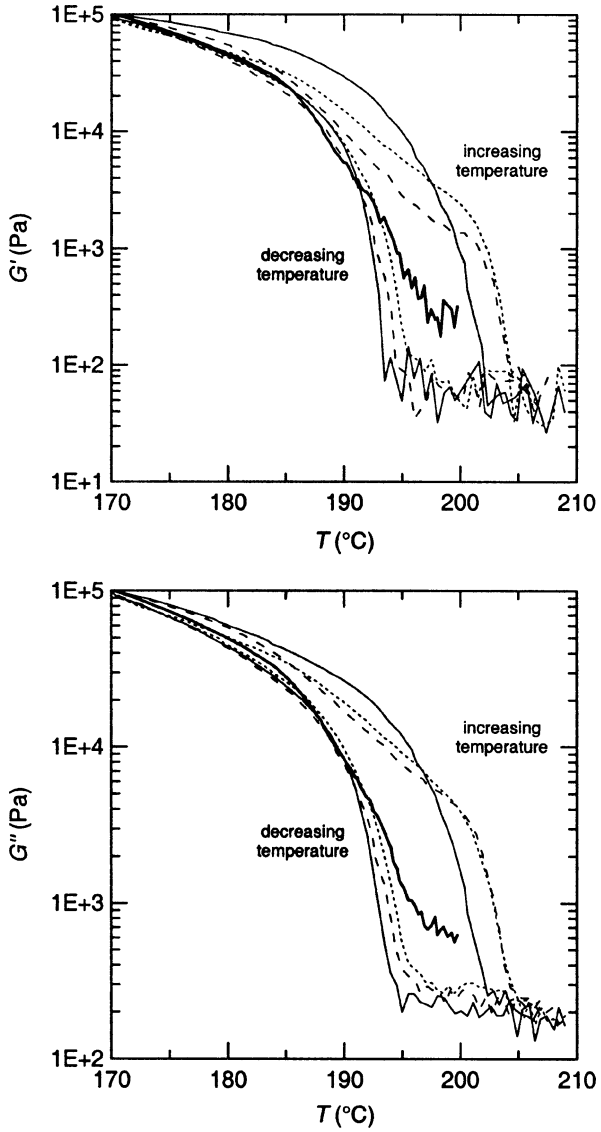

FIGURE 13 Elastic and viscous moduli of PETB as a function of temperature measured during cycles of temperature ramps from 170 to 220°C using a temperature rate of 1°C/min, a frequency of $1\,s^{-1}$, and 5% strain. Thin solid lines, first cycle applied on fresh sample; dotted lines, second cycle applied after 120 min of annealing at 194°C; dashed lines, third cycle applied after 240 min of annealing at 194°C; thick solid lines, cooling TR in a second cycle applied after 240 min of annealing at 194°C with no deformation during the first cycle or the heating TR following the annealing (see text).

place. From that temperature, G' and G'' grow steadily up to the completion of the transition to the liquid crystalline phase.

When the samples are previously exposed to an annealing process, a change in slope and an inflection point are observed in the dynamic moduli during the heating TR. This effect is more noticeable when t_A, the time extension of the annealing process, is larger. The shape of these TR curves indicate that there are two transitions during the heating ramp, that is, there are two components or regions in the polymer that have different isotropization temperatures. It is evidently the existence of a portion of material that begins the isotropization first and a portion that completes this process approximately 10°C later. It is interesting to notice the existing correspondence between the temperature range of the two zones of sharp decrease of the moduli in each curve and the temperature range of the two isotropization peaks of Figure 4. The rheological behavior observed agrees with the calorimetric results and further emphasizes the explanation that the annealing process produces the migration of molecules, which generate regions formed by materials of different molecular weights.

However, no evidence of an inflection point is observed in the cooling TR of each cycle, just a small shift of the curves that shows a gradual increment of the temperature at which the transition to the liquid crystalline organization begins. This result does not seem to agree with the DSC traces, which during the cooling portion of the cycles show two peaks in correspondence with the two isotropization transitions. The results suggest that the 20 min that the samples are kept stationery in the molten state may not be sufficient to recuperate the original molecular organization once the segregation is produced by the annealing process in the DSC, but that it is sufficient if the material is kept melted and flowing in the rheometer. The flow helps to remix the molecules and to go back to a molecular organization similar to the initial one. Examples of the influence of the imposed dynamic flow on the rheological properties of the melt have been reported in the past [12]. To reinforce this conclusion, an additional test was performed, minimizing the deformation history applied to the sample previous to the last cooling TR. That is, a fresh polymer sample was subjected to two cycles of temperature ramps. The first cycle was equivalent to the one already described for the data of Figure 13 but with no flow applied simultaneously to the sample. During the second cycle, performed after 4 h of annealing at 194°C, the temperature was raised at 1°C/min up to 205°C (instead of 220°C as before) and immediately lowered down at the same rate. No flow was applied during the heating ramp and the first portion of the cooling ramp, up to 200°C. During the rest of the cooling ramp, the dynamic moduli were measured at a frequency of $1\,s^{-1}$ and a strain of 3%. Thick solid lines in Figure 13 represent the results obtained in these conditions. In this case, the dynamic moduli measured during the cooling

TR present a change in slope and an inflection point, in agreement with the calorimetric results, and the temperature at which the transition to the liquid crystalline organization begins is higher than in the cycles with constant oscillatory shear flow. These results confirm the conclusion that the flow helps to remix the molecules and accelerates the diffusion process.

CONCLUSIONS

The polydisperse main-chain thermotropic polyester PETB presents, up to 100°C, a liquid crystalline mesophase structure of the Smectic C type. Above that temperature, the structure evolves towards a Smectic A type and remains in that condition until the temperature of isotropization is reached in the vicinity of 200°C. During the S_A-isotropic transition, a stable biphasic region is formed where the smectic and the isotropic phases coexist at equilibrium. Upon annealing at different temperatures, multimodal fusion curves are generated on the calorimetric experiments. This behavior is attributed to the preferential segregation of the lower molecular weight molecules from the liquid crystalline to the isotropic region in the biphasic zone. The enrichment of the liquid crystalline phase with the higher molecular weight fraction of the polymer progressively increases the isotropization temperature of this phase. The dependence of the isotropization temperature on the molecular weight of the polymer has been proved independently by studying the thermal behavior of three fractions of increasing molecular weight obtained by fractional precipitation of the original PETB. It has also been shown that the segregation by molecular weight generated in the biphasic zone can persist in the isotropic state for relatively long periods of time, provided that the conditions at which the polymer stays in the isotropic region avoid mechanisms other than pure diffusive migration of the segregated molecules. The rheological characterization is consistent with these results. The effect of the molecular organization and the relatively strong molecular interactions is appreciated in the low frequency regime during the anisotropic–isotropic phase transition of the polymer and at lower temperatures. The relatively large values of $G'(\omega)$ in this region indicate the presence of a weak structure that has a rheological behavior similar to that of lightly cross-linked or gel-like materials. The temperature ramps at constant frequency performed on the polymer with different thermal histories reveal that the annealing process in the biphasic zone generates two transitions on the dynamic moduli curves consistent with the existence of two phases of different molecular weight and correspondent isotropization temperatures. These effects are not evident on the cooling ramps after isotropization when the sample has been subjected to a simultaneous thermal and deformation history. This suggests that the mixing of the segregated fractions is accelerated by the oscillatory flow in the rheometer.

REFERENCES

[1] Violino, F., Alloneau, J. M., Giroud-Godquin, A., Blumstein, R. B., Stickles, E. M., & Blumstein, A. (1984). *Mol. Cryst. Liq. Cryst. Lett. Sect.*, *102*, 21.
[2] D'Allest, J. F., Wu, P. P., Violino, F., Blumstein, A., & Blumstein, R. B. (1986). *Mol. Cryst. Liq. Cryst. Lett. Sect.*, *3*, 103–115.
[3] D'Allest, J. F., Sixou, P., Blumstein, R. B., & Blumstein, A. (1988). *Mol. Cryst. Liq. Cryst.*, *157*, 229–245.
[4] Blumstein, R. B. & Blumstein, A. (1988). *Mol. Cryst. Liq. Cryst.*, *165*, 361–387.
[5] Kim, D. Y., D'Allest, J. F., Blumstein, A., & Blumstein, R. B. (1988). *Mol. Cryst. Liq. Cryst.*, *157*, 253–271.
[6] Esnault, P., Gauthier, M. M., Violino, F., D'Allest, J. F., & Blumstein, R. B. *Mol. Cryst. Liq. Cryst.*, *157*, 273–291.
[7] Laus, M., Caretti, D., Angeloni, A. S., Galli, G., & Chiellini, E. (1991). *Macromolecules*, *25*, 1459–1463.
[8] Luas, M., Angeloni, A. S., Galli, G., & Chiellini, E. (1992). *Macromolecules*, *25*, 5901–5906.
[9] Nakai, A., Wang, W., Hashimoto, T., Blumstein, A., & Maeda, Y. (1994). *Macromolecules*, *27*, 6963–6972.
[10] Nakai, A., Wang, W., Hashimoto, T., & Blumstein, A. (1996). *Macromolecules*, *29*, 5288–5296.
[11] Pérez, E., del Campo, A., Bello, A., & Benavente, R. (2000). *Macromolecules*, *33*, 3023–3030.
[12] Romo-Uribe, A., Lemmon, T. J., & Windle, A. H. (1997). *J. Rheol.*, *41*, 1117–1145.
[13] Bello, P., Bello, A., Riande, E., & Heaton, N. J. (2001). *Macromolecules*, *34*, 181–186.
[14] Bello, P., Bello, A., & Lorenzo, V. (2001). *Polymer*, *42*, 4449–4452.
[15] Bello, A., Pérez, E., Marugán, M. M., & Pereña, J. M. (1990). *Macromolecules*, *23*, 905–907.
[16] Bello, A., Riande, E., Pérez, E., Marugán, M. M., & Pereña, J. M. (1993). *Macromolecules*, *26*, 1072–1077.
[17] Ferry, J. D. (1980). *Viscoelastic Properties of Polymers*, 3rd ed. (New York: John Wiley & Sons).
[18] Gillmor, J. R., Colby, R. H., Hall, E., & Ober, C. K. (1994). *J. Rheol.*, *38*, 1623–1638.

Copyright of Molecular Crystals & Liquid Crystals is the property of Taylor & Francis Ltd and its content may not be copied or emailed to multiple sites or posted to a listserv without the copyright holder's express written permission. However, users may print, download, or email articles for individual use.